JOURNAL OF SOLID STATE CHEMISTRY 73, 235–242 (1988)

Spectroscopic Studies of Nd^{3+}-Exchanged β'' Alumina

B. DUNN AND D. L. YANG

Solid State Science Center and Department of Materials Science and Engineering, University of California at Los Angeles, Los Angeles, California 90024

AND D. VIVIEN

ENSCP, Laboratoire de Chimie Appliquée De l'Etat Solide, 11 rue Pierre et Marie Curie, 75231 Paris Cedex 05, France

Received April 20, 1987; in revised form August 14, 1987

Optical absorption spectroscopy and electron spin resonance (ESR) techniques were used to study the site occupations for Nd^{3+} in β'' alumina. In partially exchanged compositions (3.2×10^{20} Nd/cm^3) the Nd^{3+} occupy midoxygen sites primarily. There is some population of the tetrahedral site; however, the concentration is too low to be clearly observed by ESR. Crystals which were completely exchanged ($\sim 1.8 \times 10^{21}$ Nd/cm^3) exhibited rather different behavior. The spectroscopy results for these materials indicate that there is a combination of both isolated Nd^{3+} ions and discrete pairs. © 1988 Academic Press, Inc.

1. Introduction

Sodium β and β'' aluminas have long been known for their properties as solid electrolytes. The materials possess an anisotropic crystal structure which consists of spinel blocks of closely packed Al^{3+} and O^{2-} separated by loosely packed "conduction planes" which contain the mobile ionic species (i.e., Na^+) and O^{2-} (*1*). The fast ion transport properties of these materials are related to the nature of these planes. One other significant property, particularly for the β'' aluminas, is their remarkable ion-exchange behavior. Numerous divalent and trivalent ions exchange rapidly with sodium in β'' alumina, enabling a wide range of divalent and trivalent β'' alumina compositions to be synthesized (*2*). The ability to easily incorporate transition metal and lanthanide ions within β'' alumina has led to the investigation of the optical behavior of ion-exchanged β'' aluminas.

The optical properties of Nd^{3+}-exchanged β'' alumina have been investigated in some detail. Partially exchanged compositions exhibit very substantial small signal gain coefficients and lasing has been achieved in both pulsed and continuous wave modes (*3*). One of the more interesting optical properties of this material is the extremely high oscillator strength observed for the hypersensitive transition at 575 nm. A recent analysis by Alfrey *et al.* (*4*) suggested that this behavior could result from the Nd^{3+} ion occupying a midoxygen site, provided the

0022-4596/88 $3.00

ion was slightly displaced toward the column oxygen ion in the conduction plane to effectively break the inversion symmetry at the site. At this time, however, there is relatively little known about the structure of partially exchanged Nd^{3+} β'' alumina and the ion site occupations within the conduction plane. In contrast, both X-ray diffraction and transmission electron microscope (TEM) studies have been performed on fully exchanged Nd^{3+} β'' alumina. Single-crystal X-ray diffraction results indicate that the Nd^{3+} are located primarily at the (9d) or midoxygen sites in the conduction plane (*5*), and that the structure is analogous to the one reported for Gd^{3+} β'' alumina (*6*). In addition, high-resolution TEM studies have found that rare earth ions can form a three-dimensional superstructure in β'' alumina (*7*). This ordering phenomenon is apparently dependent upon heat treatment after ion exchange. The site occupation for ordered materials is rather different from that reported for the X-ray results, as Nd^{3+} was found to exhibit a significant occupation for the (6c) tetrahedral sites, also known as the Beevers–Ross (or anti-Beevers–Ross) sites.

The purpose of the present study was to use optical spectroscopy and electron spin resonance (ESR) techniques to obtain further insight concerning site populations of Nd^{3+} in β'' alumina. A partially exchanged Nd^{3+} β'' alumina, whose composition was similar to that of lasing crystals, was investigated, and the behavior was compared to that of fully exchanged Nd^{3+} β'' alumina. The results indicate that at low concentrations Nd^{3+} ions prefer the midoxygen site and that fully exchanged materials are characterized by the presence of ion pairs.

2. Experimental

The Nd^{3+} β'' alumina samples were prepared by ion-exchange techniques (*2*). In this approach, single crystals of Na^+ β'' alumina (nominally, $Na_{1.67}Mg_{0.67}Al_{10.33}O_{17}$) were grown by a flux evaporation method and then doped to different Nd^{3+} concentrations by ion-exchange procedures. The partially exchanged samples were obtained by immersing single crystals of Na^+ β'' alumina in a NaCl–$NdCl_3$ flux at 700°C for 30 min. These materials contained a Nd^{3+} concentration of approximately 3.2×10^{20} cm^{-3} and corresponded to the composition $Na_{3x}Nd_{0.56-x}Mg_{0.67}Al_{10.33}O_{17}$ with $x = 0.48$. For complete exchange, Na^+ β'' alumina crystals were placed in $NdCl_3$ melts at 800°C for 1 h. In this case the Nd^{3+} concentration was nearly 1.8×10^{21} cm^{-3} ($x \simeq 0.01$).

After exchange, the crystals were washed and dried according to the usual procedures (*2*). The extent of exchange was determined by both gravimetric and X-ray absorption techniques. These synthesis methods did not include any extended annealing treatments and would not be expected to produce the highly ordered structures discussed by Davies *et al.* (*7*), but rather correspond to "quenched" materials. Optical absorption spectra between 250 and 2000 nm were taken over the temperature range 4 to 300°K using an Oxford Instruments cryostat in conjunction with a Beckman 5270 UV spectrometer. The ESR measurements were made at *X* band using a Bruker 220D spectrometer equipped with an Oxford Instruments helium flow cryostat. The data were acquired at 20°K because of the relatively short spin lattice relaxation time of the Nd^{3+} ion.

3. Results

3.1. Optical Absorption

The optical spectra for the partially exchanged materials were such that the various optical transitions for an isolated Nd^{3+} ion could be readily identified. The $^4I_{9/2} \rightarrow {}^2P_{1/2}$ transition (420–430 nm) at liquid helium temperatures is of most interest because the number of absorption lines gives the number of Nd^{3+} sites in the structure. The $^2P_{1/2}$ level is not split by the crystal field ($J + \frac{1}{2} = 1$) and, therefore, at low temperatures, when only the lowest $^4I_{9/2}$ Stark level is populated, there will be a single line for each Nd^{3+} site. Figure 1a indicates the presence of two distinct lines at 427 and 430 nm suggesting that Nd^{3+} occupies two sites in β″ alumina. Other transitions in the optical spectra are consistent with the $^4I_{9/2} \rightarrow {}^2P_{1/2}$ result. That is, the transitions exhibit more components than would be expected if only one site was occupied. In most cases, however, the lines for a given transition show considerable overlap and it is difficult to observe all the lines expected for two sites. An example of this overlap is shown in Fig. 2a for the hypersensitive $^4I_{9/2} \rightarrow {}^4G_{5/2}, {}^2G_{7/2}$ transition. There are more than the seven lines expected for one Nd^{3+} site, but it is difficult to clearly identify all the components expected for two sites. We have also investigated the temperature dependence of the $^4I_{9/2} \rightarrow {}^2P_{1/2}$ transition and found that this transition is rather independent of temperature. Over the temperature range 4–300°K the two peaks exhibited only slight broadening and no change in their relative ratio.

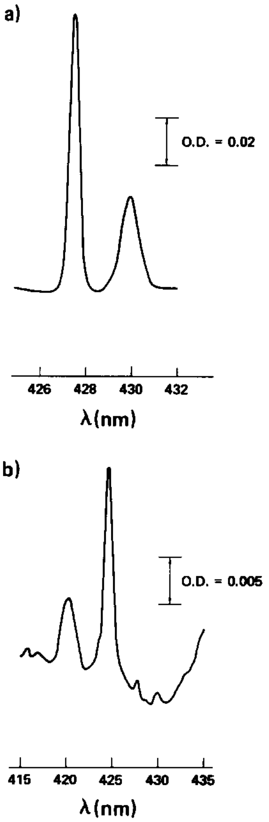

FIG. 1. Absorption spectrum of Nd^{3+} β″ alumina at 4.2°K for the $^4I_{9/2} \rightarrow {}^2P_{1/2}$ transition. The beam (unpolarized) was propagating along the $\bar{c}$ direction. (a) Low Nd^{3+} concentration, 3.2×10^{20} cm^{-3} sample thickness = 0.04 cm; (b) high Nd^{3+} concentration, 1.8×10^{21} cm^{-3} sample thickness = 0.03 cm.

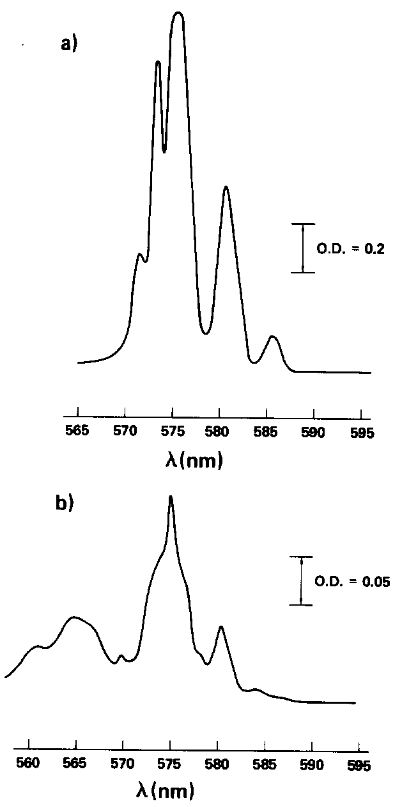

FIG. 2. Absorption spectrum of Nd^{+3} β″ alumina at 4.2°K for the $^4I_{9/2} \rightarrow {}^4G_{5/2}, {}^2G_{7/2}$ transition. The beam (unpolarized) was propagating along the $\bar{c}$ direction. (a) Low Nd^{3+} concentration; (b) high Nd^{3+} concentration.

The high concentration Nd^{3+} β'' alumina crystals show distinctly different behavior. The ${}^4I_{9/2} \rightarrow {}^2P_{1/2}$ transition exhibits two new lines at 424.5 and 420 nm. (Fig. 1b). Both of these lines are shifted to shorter wavelengths than the peaks observed for partially exchanged β'' alumina in Fig. 1a. The original peaks are still evident, but they are extremely weak. The trend to have new groups of lines at shorter wavelengths is also apparent for other transitions. The hypersensitive transition (Fig. 2b) exhibits new lines and considerable broadening toward the shorter wavelengths (560–570 nm). In the 585–570-nm range, the spectra are comparable, although the absorption intensity for the fully exchanged Nd^{3+} β'' alumina is greatly reduced.

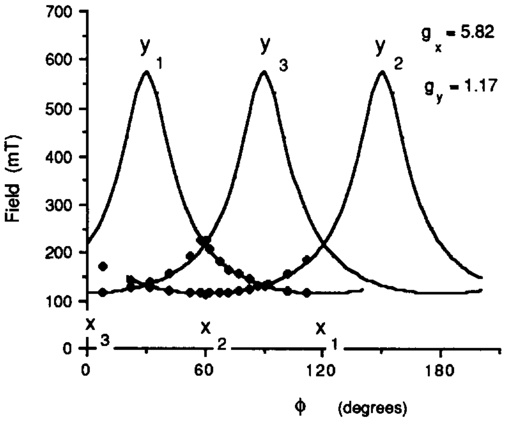

FIG. 3. Angular variation of the ESR signal for Nd^{3+} β'' alumina (low concentration). The applied magnetic field is in the *ab* plane. The experimental points are indicated. There are three crystallographically equivalent sites in the *ab* plane whose *x* and *y* *g*-tensor axes are shown, taking ϕ $(x_3) = 0$.

3.2. ESR

The Nd^{3+} ion behaves as an ion with fictive spin $S' = \frac{1}{2}$ (only the lowest Kramers doublet of the ${}^4I_{9/2}$ is populated at 20°K). The spectra for a crystal containing isolated Nd^{3+} ions will consist of a central line for each Nd^{3+} site plus hyperfine satellites due to ${}^{143}Nd$ and ${}^{145}Nd$ isotopes of nuclear spin $\frac{7}{2}$ (natural abundance 12.7 and 8.3%, respectively). For samples with low dopant concentration, only central lines are observed. The linewidth is quite broad, generally greater than 25 mT, and this prevents observation of the hyperfine interaction.

Figure 3 shows the angular variation of the ESR signal in the *ab* plane (i.e., $B_0 \perp c$) for partially exchanged Nd^{3+} β'' alumina. The lines are calculated from the formula for an orthorhombic site,

$$g^2(\theta, \phi) = [lg_x]^2 + [mg_y]^2 + [ng_z]^2, \quad (1)$$

where l, m, and n are the direction cosines of B_0 with respect to the *g*-tensor axes. Eq. (1) is valid for one site, and it is apparent that it satisfies all the experimentally obtained points. Three lines are expected to arise corresponding to sites 1, 2, and 3 in the *ab* plane. These three sites are crystallographically equivalent but their *g*-tensor axes (which we attribute to being the *x*- and *y*-axes of the *g*-tensor, and along which one line should be at its extremum in field) are rotated by 120° from each other. These three lines with the corresponding g_x and g_y values are indicated in Fig. 3. Experimentally, we observed only one or two lines for each value of ϕ. The reason is that the linewidth for $B_0 > 240$ mT was greater than 25 mT and we were, therefore, unable to extract any additional information from the background. The dependence of linewidth on the magnetic field is shown in Fig. 4. From the data and the curves in Fig. 3, we are able to establish that $g_x = 5.82$ and $g_y = 1.17$. The latter value represents a best fit using the calculated curve.

The third *g* parameter, g_z, can be determined from the angular variation of the ESR signal in a plane containing the *c*-axis. The data are shown in Fig. 5 where it is evident that all three lines could be observed. As the crystal was turned toward the *c*-axis (i.e., as B_0 became parallel to the *c*-axis), the field became far too large to be measured by the spectrometer, and it was not possible to ob-

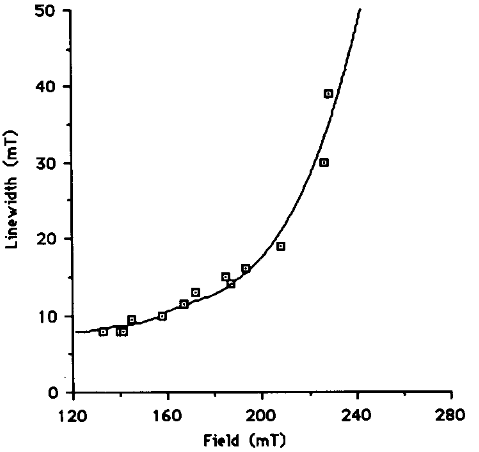

FIG. 4. The linewidth for the ESR signals shown in Fig. 3 as a function of the applied magnetic field.

tain a value for g_z experimentally. The fact that this line is an extremum suggests that the c-axis must correspond to g_z (i.e., g_x and g_y are in the ab plane). Each of the three lines in Fig. 5 corresponds to one of the lines in Fig. 3 taken at a constant value of ϕ. The specific values of ϕ were determined by comparing the values in Fig. 5 at $\theta = 90°$ (i.e., the ab plane) with the observed angular variation in the ab plane (Fig. 3). It was found, as expected, that the values at $\phi = 90°$ fit along a single vertical in Fig. 3 which thus identified the ϕ values associated with each of the lines in Fig. 5.

The inability to measure g_z directly requires that we compute it using Eq. (1). Although we know the appropriate values of g_x, g_y, ϕ, and θ, we find that fitting the lines in Fig. 5 is extremely sensitive to the accuracy of these values. It is evident that g_z has a value close to zero. In fact, when we substitute $g_z = 0$ in Eq. (1), the curves for $g(\theta)$ at constant ϕ (Fig. 5) fit the experimental data away from the c-axis rather well. Unfortunately, in the region closer to the c-axis ($\theta < 30°$) this is not the case. Attempts were made to fit the $g(\theta)$ data by using a series of g_z values close to zero. These calculations, however, could not be optimized successfully because of extreme sensitivity to the parameters in Eq. (1). Thus, at the present time, we are unable to ascertain a precise value for g_z, other than to indicate that it is a value close to zero. Nonetheless, for the purpose of the current investigation, where we are interested in structural information such as the site and symmetry of Nd^{3+}, these ESR results are still quite useful to us.

In addition to the measurements at 20°K, the ESR spectra were taken over a range of temperature. At temperatures above 50°K, the spin lattice relaxation time had shortened sufficiently so that the linewidth increased greatly. The ESR line was no longer evident above 70°K.

The fully exchanged Nd^{3+} β'' alumina exhibited rather different behavior as compared to the partially exchanged materials. We determined the angular variation for the ESR line when B_0 was turned in a plane containing the c-axis and found that some of the points exhibited a similar angular variation to that obtained for the lower Nd^{3+} concentration sample shown in Fig. 5. However, there were many other points which either displayed no angular variation or, in contrast, a very substantial one. As a result,

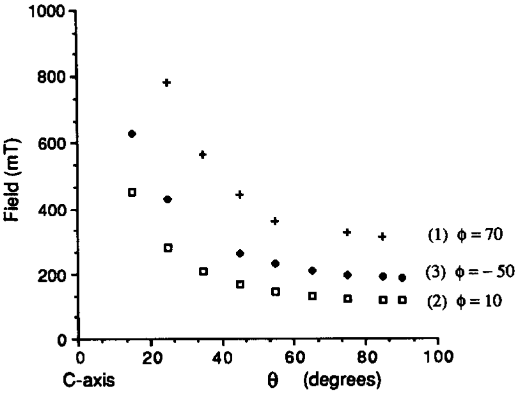

FIG. 5. Angular variation of the ESR signal for Nd^{3+} β'' alumina (low concentration) where the magnetic field is applied in a plane containing the c-axis. The orientation of the c-axis is shown. The three sites correlate with those indicated in Fig. 3.

the ESR spectra were too complicated to interpret meaningfully. The linewidths for these materials were also quite broad and, once again, it was not possible to observe the hyperfine interaction.

4. Discussion

4.1. Partially Exchanged Nd^{3+} β'' Alumina.

The spectroscopy results offer a fairly consistent interpretation regarding the site occupancy of Nd^{3+} ions in β'' alumina for the partially exchanged compositions. The optical absorption measurements indicate Nd^{3+} is present in two sites. Using the explanation developed by Caro *et al.* (*8, 9*) for the nephelauxetic effect for Nd^{3+}, it is possible to associate these lines with Nd^{3+} site populations. Caro and Derouet (*8*) related the coordination number for Nd^{3+} and the Nd–O distance to the position of the $^2P_{1/2}$ level. In general, a larger Nd–O distance and coordination number produce an absorption line at shorter wavelengths. In β'' alumina, the octahedral (mO) site will be characterized by larger Nd–O distances than the tetrahedral (BR or aBR) sites. Therefore, one expects the line at 427 nm to correspond to Nd^{3+} present in mO sites while the line at 430 nm corresponds to the occupation of the BR (or aBR) site.

The ESR data provide complementary information regarding the site distributions. The fact that all the ESR lines can be explained by the use of Eq. (1) indicates that the Nd^{3+} are located in a single site. Since the intensity of the ESR signal is known to be proportional to the concentration of a given species, if Nd^{3+} ions occupy a second site (whose signal may be hidden by the broad linewidth), the concentration must be rather small. Significantly, the ESR results also identify the nature of the predominant site. Figure 3 clearly indicates that the g parameters in the *ab* plane are not equal and that the Nd^{3+} ions lie in an orthorhombic site. This behavior is consistent for Nd^{3+} ions located in the octahedral mO positions which are characterized by C_{2h} symmetry. In contrast, BR sites possess C_{3v} symmetry. If such sites were occupied, the ESR spectrum would be characterized by axial symmetry, with the axis along the $\bar{c}$ direction. It is evident from our present investigation that the Nd^{3+} ions in β'' alumina do not reside in tetrahedral sites.

A previous spectroscopy study by Alfrey *et al.* (*4, 10*), performed on crystals of similar Nd^{3+} concentration, reached analogous conclusions. Using a Judd–Ofelt analysis of the absorption spectrum intensities, Alfrey *et al.* proposed that the anomalously high oscillator strength of the hypersensitive transition resulted (in part) from Nd^{3+} ions being somewhat displaced (by 0.1–0.2 Å) from the midoxygen site. In addition, based upon a more detailed analysis of the optical transitions, they suggested that Nd^{3+} was probably located in more than one site. In the present study, we find rather direct evidence for both of these features. It is clear that Nd^{3+} ions populate two sites, and that the midoxygen site is dominant. It is also significant to note that the results described here are consistent with those obtained from X-ray diffraction studies on completely exchanged compositions (*5*).

One notable feature regarding the temperature dependence of the optical spectra is the fact that only slight changes were observed over the range 4 to 300°K. This suggests that the first Stark level of the $^4I_{9/2}$ is widely separated from the next level. Such behavior is fairly consistent with the ESR spectra, where the lines were found to disappear at temperatures (70°K) which are rather high for Nd^{3+} ions.

At the present level of investigation and without additional information regarding the wave functions of different levels, it is not possible to provide a more detailed interpretation of the ESR transitions. Nonetheless, we are able to compare our results with the large number of previous investigations which correlate *g* values and symmetry considerations. The *g* values obtained in the current study are not unusual for Nd^{3+}. Similar results were reported for Nd^{3+} in $CaO{-}2Al_2O_3$ (*11*) and Y_2O_3 (*12*) hosts. Both cases are particularly relevant to the present work because the Nd^{3+} were found to reside in C_2 sites. The significance here is that a C_2 site is expected in β'' alumina when Nd^{3+} are displaced slightly away from the center of the mO site. Such displacements were proposed by Alfrey *et al.* (*4*) to account for the optical absorption of the hyperfine transition.

4.2. Completely Exchanged Nd^{3+} β'' Alumina

In general, the completely exchanged Nd^{3+} β'' alumina compositions are quite different spectroscopically from the partially exchanged materials. This difference is particularly evident in the ESR spectra where it appears that magnetic pairing occurs. The angular dependence for some of the ESR lines is comparable to the low concentration samples and thus represents the presence of isolated Nd^{3+} ions which are unperturbed. However, it is also quite apparent that new species are present. The nature of the lineshape suggests that we do not have Nd^{3+} clusters. Instead, there seem to be sets of discrete pairs. The magnetic axes for the Nd^{3+} pairs are within the conduction plane. These pairs would be expected to give rise to a number of different angular dependencies, as observed experimentally.

The existence of Nd^{3+} pairs may be responsible for the changes observed in the optical spectra (Figs. 1 and 2). The two lines observed at 424.5 and 420 nm are at too high energy to be the $^4I_{9/2} \rightarrow {}^2P_{1/2}$ transition of isolated ions (*8*). This is an indication that the peaks correspond to another type of Nd^{3+} species. Pairs of interacting Nd^{3+} ions will give rise to new levels. If some of the new levels develop at higher energies, then the combination of isolated Nd^{3+} ions and Nd^{3+} pairs would be able to account for the changes which occur in the optical spectra of the concentrated Nd^{3+} samples. However, it must also be recognized that the magnetic interactions observed from ESR may not necessarily be associated with the changes that result from optical transitions.

5. Conclusions

Optical absorption and ESR measurements were used to identify site occupations for Nd^{3+} in β'' alumina. For partially exchanged samples, Nd^{3+} ions are located primarily on midoxygen sites with some occupancy of a second site. No detailed information regarding the location of the second site was obtained. The temperature dependence of the optical absorption indicated that the separation of the Stark levels of the $^4I_{9/2}$ are sufficiently wide that only the lowest level is occupied. The crystals containing high Nd^{3+} concentration exhibited rather different behavior. The presence of discrete Nd^{3+} pairs is suggested and the ESR spectra indicated that fully exchanged Nd^{3+} β'' alumina contained a combination of discrete pairs and isolated Nd^{3+} ions.

Acknowledgments

The work was supported in part by the U.S. Office of Naval Research and the Franco-American Commission for Cultural Exchange. Helpful discussions with Professor O. M. Stafsudd are greatly appreciated. The authors thank D. Simons and B. Schwarz for their experimental assistance.

References

1. R. Collongues, D. Gourier, A. Kahn, J. P. Boilot, Ph. Colomban, and A. Wicker, *J. Phys. Chem. Solids* **45**, 981 (1984).
2. B. Dunn and G. C. Farrington, *Solid State Ionics* **18, 19**, 31 (1986).
3. M. Jansen, A. J. Alfrey, O. M. Stafsudd, D. L. Yang, B. Dunn, and G. C. Farrington, *Opt. Lett.* **9**, 119 (1984).

4. A. J. Alfrey, O. M. Stafsudd, D. L. Yang, B. Dunn, and L. Salmon, submitted for publication.
5. B. Dunn, J. O. Thomas, and G. C. Farrington, *in* "Spectral Properties of Solid-State Laser Type Materials" (B. D. Bartolo, Ed.), Plenum, New York, in press.
6. W. Carillo-Cabrera, J. O. Thomas, and G. C. Farrington, *Solid State Ionics* **9, 10,** 245 (1983).
7. P. Davies, A. Petford, and M. O'Keefe, *Solid State Ionics* **18, 19,** 624 (1986).
8. P. Caro and J. Derouet, *Bull. Soc. Chim. France* **1,** 46 (1972).
9. P. Caro, O. Beaury, and E. Antic, *J. Phys.* **37,** 671 (1976).
10. A. Alfrey, Ph.D. Thesis, University of California, Los Angeles (1985).
11. A. J. Lindop and D. W. Goodin, *J. Phys. C.* **6,** 1818 (1973).
12. K. H. Hellwege, S. Hufner, G. Schafer, and S. Scheller, *Phys. Kondens. Mater.* **6,** 100 (1967).